

Probing Heavy Ion Collisions Using Quark and Gluon Jet Substructure

Yang-Ting Chien

LHC Theory Initiative Fellow, MIT Center for Theoretical Physics

In collaboration with Raghav Kunnawalkam Elayavalli
arXiv:1803.03589

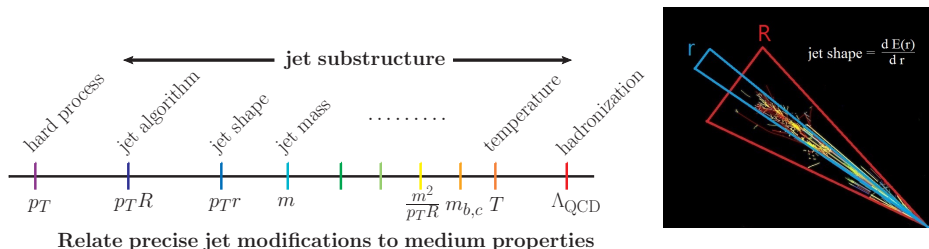
June 12, 2018, RHIC & AGS Users Meeting

Outline

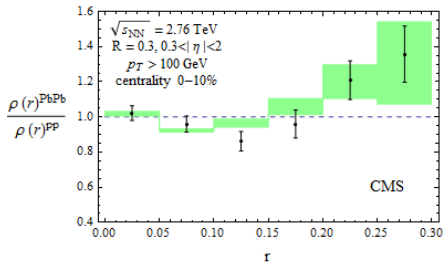
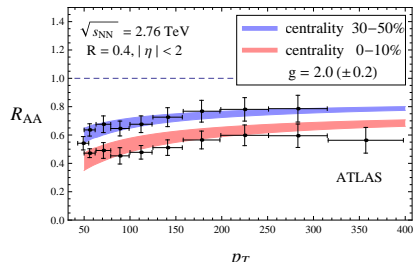
- ▶ Jet substructure: hard and soft probes at all energy scales
- ▶ Quark and gluon jets as two different probes
- ▶ Jet representation and analysis
 - ▶ physics-motivated multivariate analysis: constructive
 - ▶ unbiased machine-learning features: comprehensive
- ▶ Telescoping deconstruction: a complete jet observable basis
 - ▶ subjet, soft-drop and collinear-drop
- ▶ Conclusion

The era of precision jet substructure studies

SCET Chien-Vitev JHEP05(2016)023



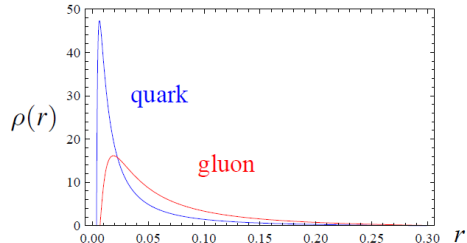
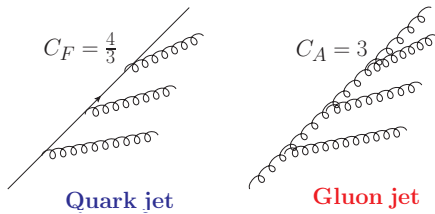
Relate precise jet modifications to medium properties



Two more jet workshops at BNL coming up!



Quark jets and gluon jets



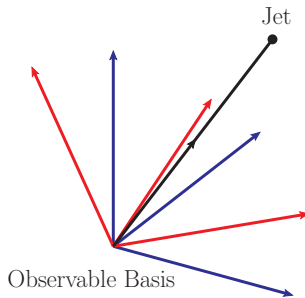
- ▶ All the jets are a mixture of quark jets and gluon jets
- ▶ Quark and gluon jets have different color charges and substructure
- ▶ Quark/gluon jet fraction affects jet substructure
 - ▶ 40% quark 60% gluon → 60% quark 40% gluon: jets become more quark-jet like
- ▶ Substructure of each jet is modified
 - ▶ Quark jets and gluon jets are modified differently

Use quark jets and gluon jets as independent probes



- ▶ Classify quark jets and gluon jets in pp and AA
- ▶ Distinguish pp jets from AA jets
 - ▶ identify **all** jet features which encode **all** jet modifications
- ▶ Closely related to quark/gluon discrimination
 - ▶ highlight quark and gluon jet differences

Jet representations

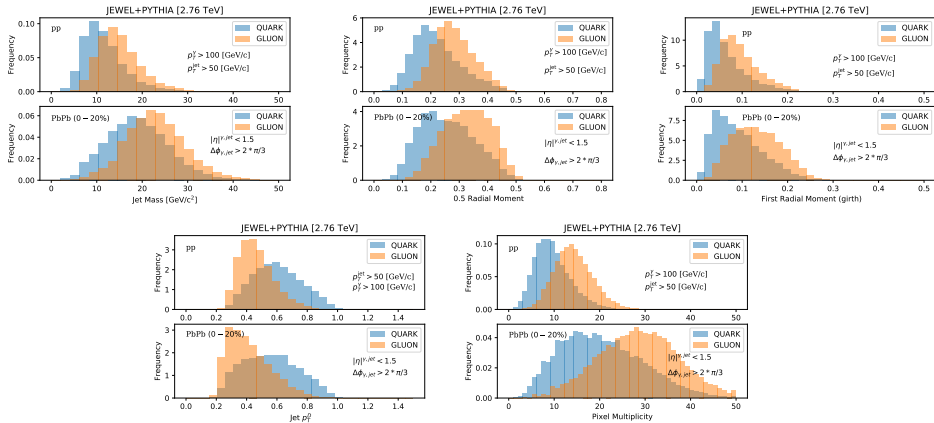


- ▶ Different multivariate techniques suit different jet representations
 - ▶ list of physics-motivated observables
 - ▶ unbiased and raw input
 - ▶ complete basis and expansion
- ▶ Modern computation power and deep learning tools help benchmark jet feature identification

- ▶ Illustrate using supervised learning in classification task
- ▶ Quark and gluon enriched jet samples are generated from Monte Carlo simulations
 - ▶ e.g. using JEWEL $q + \gamma$ and $g + \gamma$ channels (Zapp et al)
 - ▶ methods applicable to all simulations and experimentally quark/gluon-enriched data

Physics-motivated multivariate analysis

- ▶ Representative variables capturing quark and gluon jet features
- ▶ Exploiting observable correlations in high-dimensional space
- ▶ jet mass and radial moments $\sum_i p_T^i \Delta\theta_{jet,i}^\kappa / p_T^{\text{jet}}$ with $\kappa = 0.5, 1$
- ▶ $p_T^D = \sqrt{\sum_i p_T^i} / p_T^{\text{jet}}$ and pixel multiplicity



Jet image

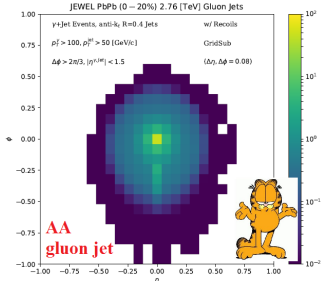
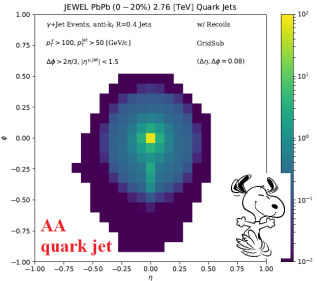
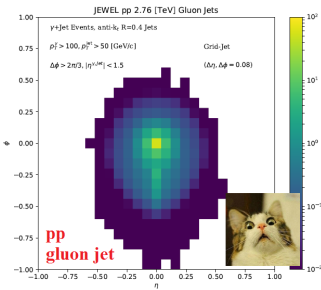
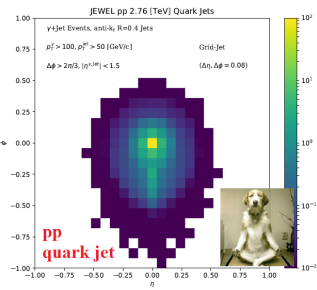
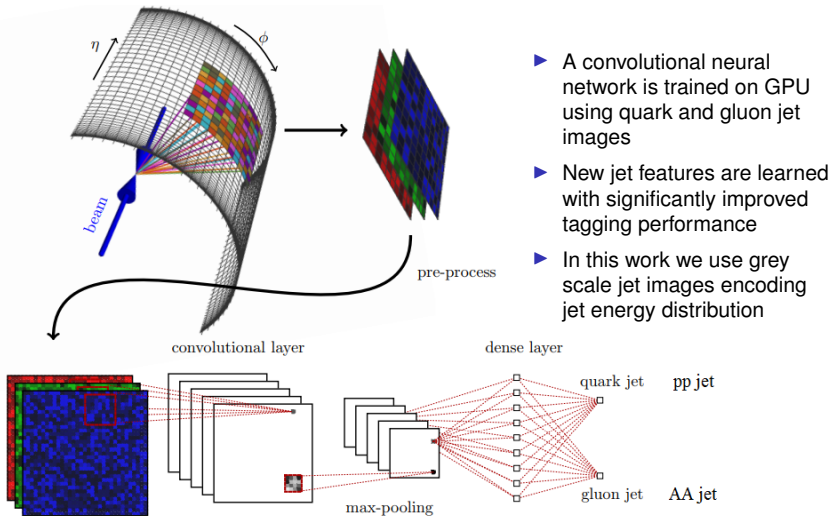


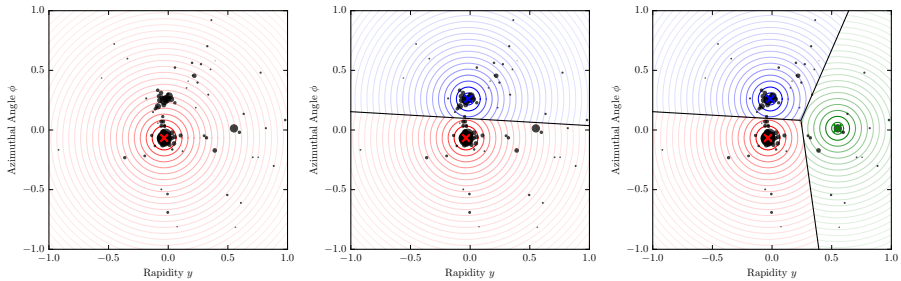
Image recognition using convolutional neural network



Schwartz et al, Deep learning in color, JHEP01(2017)110

Telescoping Deconstruction: a complete subjet fragmentation basis

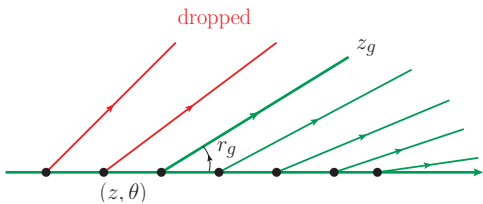
- ▶ A fixed-order N subjet expansion with subjet kinematics
 - ▶ identify dominant energy flow directions using N soft recoil-free axes
 - ▶ reconstruct subjets around the axes with multiple subjet radii R
 - ▶ TD observables represent *subjet topology* and *subjet substructure*
- ▶ Closely related to perturbative expansion and parton shower picture



Chien et al, arXiv:1711.11041

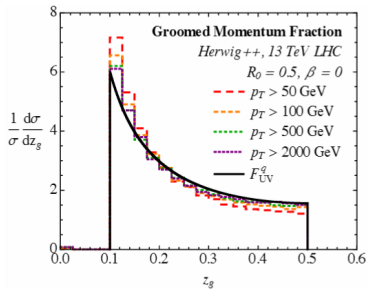
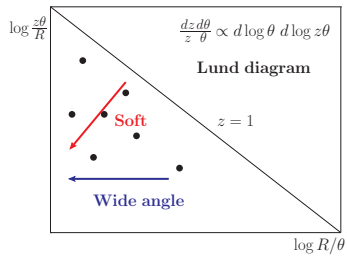
Subjet distribution, soft drop, and Lund diagram

Soft drop, Thaler et al, JHEP05(2014)146



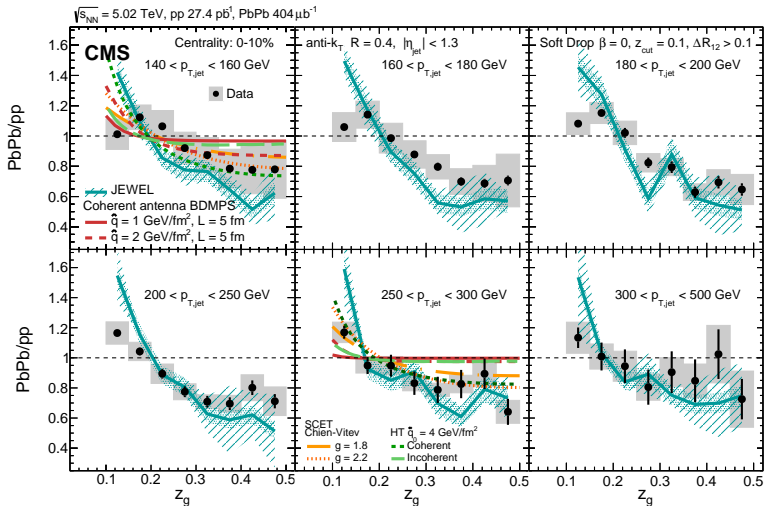
- ▶ C/A tree-based procedure to drop soft radiation
- ▶ Soft-drop condition

$$z < z_{\text{cut}} \theta^{\beta}, z = \frac{\min(p_{T1}, p_{T2})}{p_{T1} + p_{T2}}$$
- ▶ Lund diagram encodes branching kinematics along hard branches

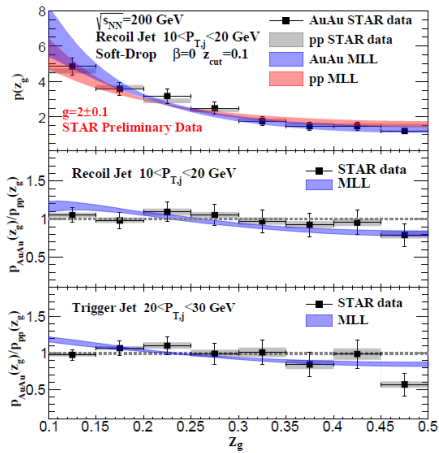


Modification of z_g at the LHC

SCET Chien-Vitev PRL 119 (2017) 112301, CMS PRL 120 (2018) 142302



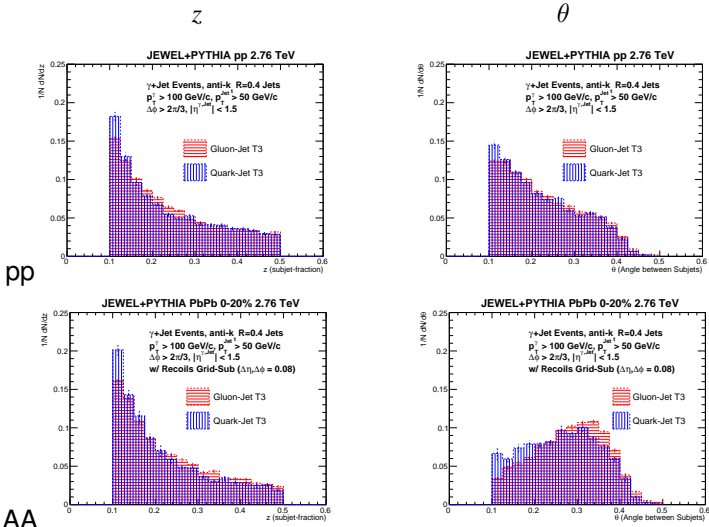
Modification of z_g at RHIC



Li & Vitev 1801.00008

Telescoping subjet topology

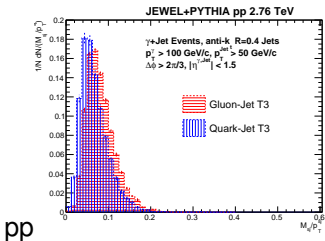
- Enhancement of soft, wide angle radiation



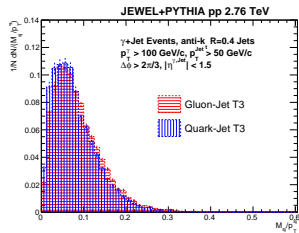
Telescoping subjet substructure

- Reveal subjet flavor dependence in first splitting $q \rightarrow qg$ and $g \rightarrow gg$ using $m^{\text{sub}}/p_T^{\text{sub}}$

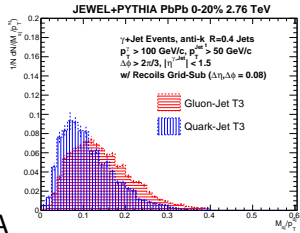
Hard Subjet



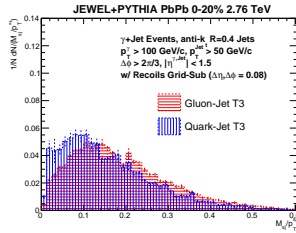
Soft Subjet



pp

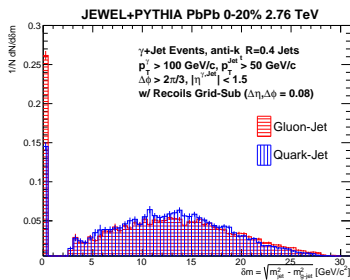
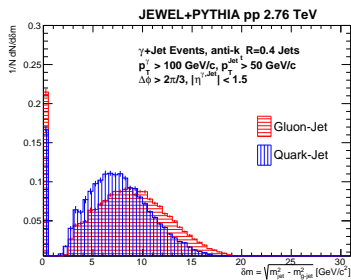


AA



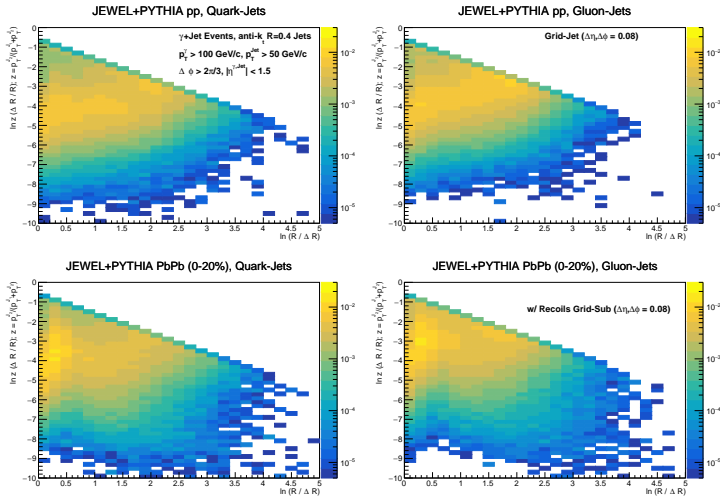
Collinear-drop: probing soft-dropped radiation

- ▶ Variation of m^2 between ungroomed and groomed jets: $\delta m = \sqrt{m_{\text{ungroomed}}^2 - m_{\text{groomed}}^2}$
- ▶ Quark/gluon jet difference disappearing in AA collisions



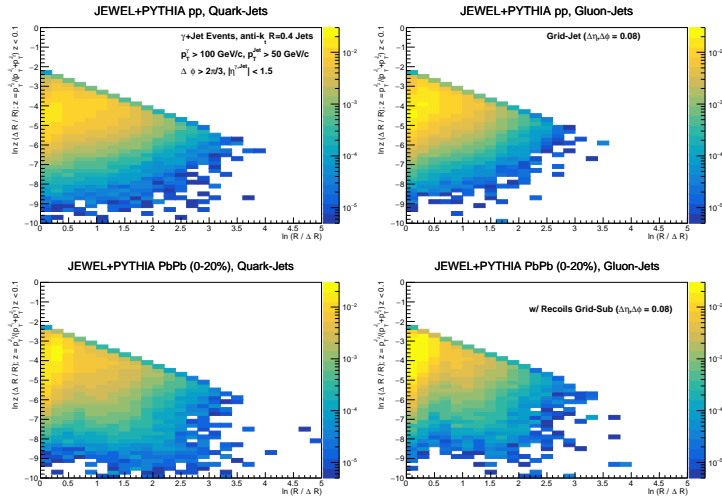
Lund diagram

- Significant increase of wide angle, soft radiation in AA



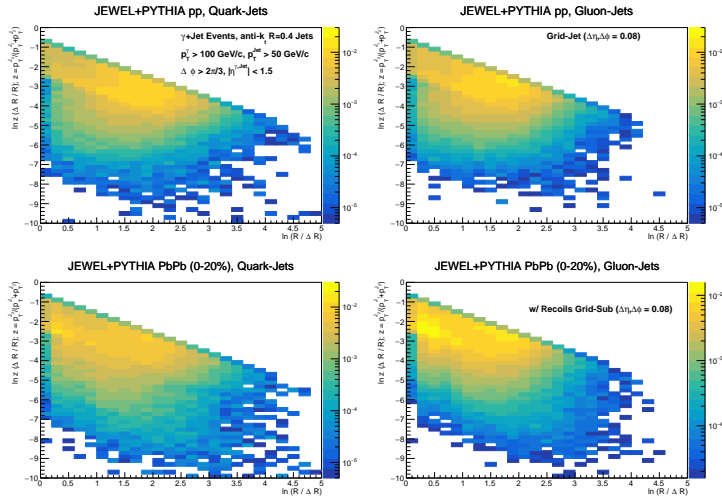
Lund diagram, soft-dropped radiation

- Much wide angle, soft radiation is removed (soft-drop $\beta = 0$, $z_{\text{cut}} = 0.1$)

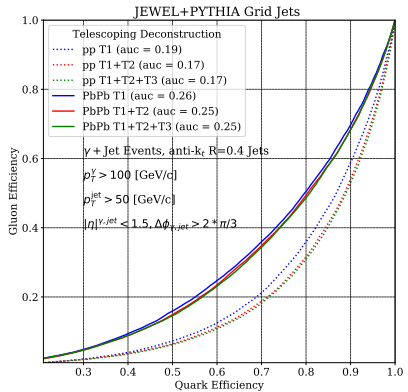
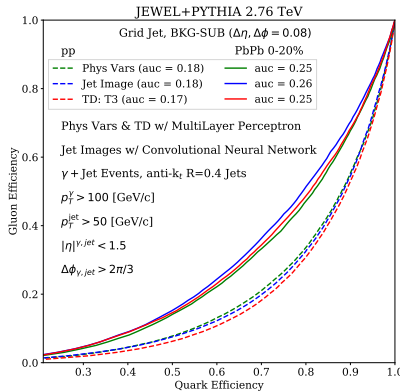


Lund diagram, hard branch

- Significant soft radiation still remains within the hard branch (soft-drop $\beta = 0$, $z_{\text{cut}} = 0.1$)

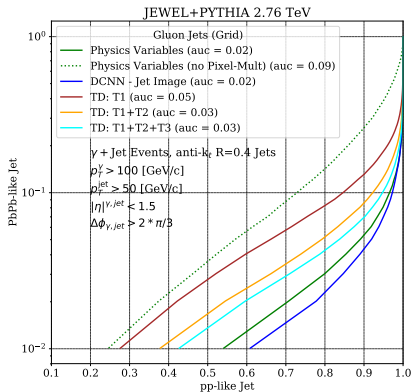
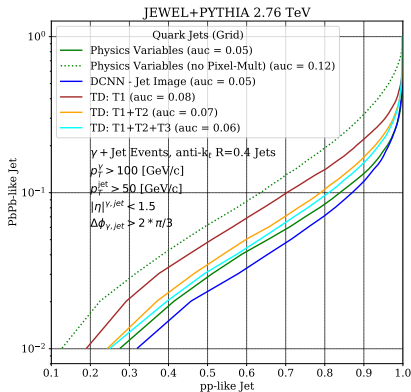


Quark gluon jet classification



- ▶ ROC curves: the lower the curve, the better the performance
- ▶ Performance drops in heavy ion collisions
- ▶ Information contained in subleading subjets is washed out in JEWEL

pp and AA jet classification



- ▶ Gluon jets are modified more than quark jets
- ▶ Pixel multiplicity is the dominant feature distinguishing pp and AA jets in JEWEL

Conclusion

- ▶ Quark and gluon jet classification provides a new method of studying jet modification
- ▶ Modifications of collective jet substructure observables provide qualitatively new insights
- ▶ Machine-learning techniques are powerful tools in jet modification studies
- ▶ Quark/gluon classification performance drops in JEWEL-simulated AA collisions
- ▶ Telescoping deconstruction provides a complete and systematic jet substructure framework
- ▶ Jet modification inverse problem: complete jet substructure studies will teach us the inner working of QGP

Bonus slides

Power counting for δm^2 in SCET

- $\delta m^2 = m^2(\text{ungroomed}) - m^2(\text{sd})$ with soft-drop parameters $\beta = 0, z_{\text{cut}} = 0.1$

- ▶ In-jet global soft mode

$$p_s = E_J z_{\text{cut}}(1, R^2, R), \text{ with } \mu_s = E_J R z_{\text{cut}}$$

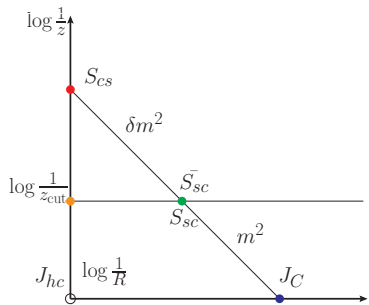
- ▶ Soft-collinear mode

$$p_{sc} = (E_J z_{\text{cut}}, \frac{\delta m^2}{2E_J}, \sqrt{\frac{z_{\text{cut}} \delta m^2}{2}}), \text{ with } \mu_{sc} = \sqrt{\frac{z_{\text{cut}} \delta m^2}{2}}$$

- ▶ C-soft mode

$$p_{cs} = (\frac{\delta m^2}{2E_J R^2}, \frac{\delta m^2}{2E_J}, \frac{\delta m^2}{2E_J R}), \text{ with } \mu_{cs} = \frac{\delta m^2}{2E_J R}$$

▶ $\mu_s \gg \mu_{sc} \gg \mu_{cs}, \delta m^2 \approx m^2$



Factorization of δm^2

- ▶ Factorization of soft-drop jet mass

$$J^\delta(m^2, \mu) = \int dp^2 dk J(p^2, \mu) S^\delta(k, R, z_{cut}, \mu) \delta(m^2 - p^2 - 2E_J k)$$

where $S^\delta(k, R, z_{cut}, \mu) = S_C(k, R, z_{cut}, \mu) S_G(R, z_{cut}, \mu)$

- ▶ With the measurement of δm^2 , the in-jet global soft sector is constrained and needs to be refactorized

$$S_G(R, z_{cut}, \mu) \rightarrow S(k_1, R, z_{cut}, \mu) = \int dk_2 dk_3 S_{in}(k_2, R, \mu) \overline{S_C}(k_3, R, z_{cut}, \mu) \delta(k_1 - k_2 - k_3)$$

where $\overline{S_C}$ is the complement of S_C

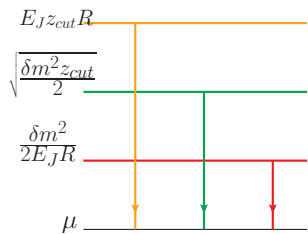
- ▶ Soft-drop jet mass is integrated out and gives soft-drop unmeasured jet function

$$\frac{d\sigma}{d\delta m^2} = \frac{J_{un}^{sd}(\mu) S\left(\frac{\delta m^2}{2E_J}, R, z_{cut}, \mu\right)}{J_{un}(\mu)} = \frac{S\left(\frac{\delta m^2}{2E_J}, R, z_{cut}, \mu\right)}{S_G(R, z_{cut}, \mu)}, \quad \text{RG invariant}$$

Anomalous dimensions and RG evolution

- Large logarithms of $\delta m^2/E_J$ are resummed using RG evolution

$$\frac{d\tilde{S}(\nu, \mu)}{d \ln \mu} = \gamma(\mu) \tilde{S}(\nu, \mu), \text{ where } \tilde{S}(Q^2, \mu) = \int dk \exp \left(-\frac{2E_J}{Q^2 e^{\gamma_E}} \right) S(k, \mu)$$



$$\gamma_{S_G}(\mu) = 2C_i \Gamma_{cusp} \ln \frac{\mu}{2E_J z_{cut} \tan \frac{R}{2}} + \gamma^s$$

$$\gamma_{S_{\overline{S}_C}}(\mu) = -2C_i \Gamma_{cusp} \ln \frac{Q^2 z_{cut}}{\mu^2} + \gamma_c^s$$

$$\gamma_{S_{in}}(\mu) = 2C_i \Gamma_{cusp} \ln \frac{Q^2}{\mu 2E_J \tan \frac{R}{2}} + \gamma_{in}^s$$

$$\gamma_{S_G}(\mu) = \gamma_{S_{in}}(\mu) + \gamma_{S_{\overline{S}_C}}(\mu)$$

Resummed and fixed-order δm^2 (preliminary)

- At $\mathcal{O}(\alpha_s)$,

$$\frac{d\sigma}{d\delta m^2} = \frac{\alpha_s C_i}{\pi \delta m^2} \ln \frac{z_{cut} E_J^2 R^2}{\delta m^2}$$

- At NLL,

$$\begin{aligned} \frac{d\sigma}{d\delta m^2} &= \exp \left[2C_i S(\mu_{cs}, \mu_{sc}) + 2C_i S(\mu_{sc}, \mu_s) + 2A_s(\mu_{sc}, \mu_s) + 2A_s(\mu_{cs}, \mu_s) \right] \\ &\quad \times \left(\frac{\mu_{sc}^2}{\mu_s \mu_{cs}} \right)^{-2C_i A_\Gamma(\mu_{cs}, \mu_{sc})} \left(\frac{\mu_s}{2E_J z_{cut} \tan \frac{R}{2}} \right)^{-2C_i A_\Gamma(\mu_{cs}, \mu_s)} \frac{1}{\delta m^2 S_G(\mu_s)} \\ &\quad \tilde{S}_C(\partial\eta, \mu_{sc}) \tilde{S}_{in}(\partial\eta + \ln \frac{\mu_{sc}^2}{\mu_{cs}(2E_J z_{cut} \tan \frac{R}{2})}, \mu_{cs}) \left(\frac{\delta m^2 z_{cut}}{\mu_{sc}^2} \right)^\eta \frac{e^{-\gamma_E \eta}}{\Gamma(\eta)} \end{aligned}$$

where $\eta = -2C_i A_\Gamma(\mu_{cs}, \mu_{sc})$. $S(\mu_1, \mu_2)$ and $A(\mu_1, \mu_2)$ are RG evolution kernels.

Plots

- ▶ Non perturbative contributions are significant: opportunity to probe medium-scale physics, and a challenge!

